

# Microgels containing methacrylic acid: effects of composition on pH-triggered swelling and gelation behaviours

Sarah Lally · Robert Bird · Tony J. Freemont ·  
Brian R. Saunders

Received: 22 October 2008 / Revised: 14 December 2008 / Accepted: 18 December 2008 / Published online: 22 January 2009  
© Springer-Verlag 2009

**Abstract** pH-responsive microgels are cross-linked polymer colloids that swell when the pH approaches the  $pK_a$  of the particles. In this work, we present a comprehensive investigation of pH-triggered particle swelling and gel formation for a range of microgels containing methacrylic acid (MAA). The microgels investigated have the general composition poly(A/MAA/X), where A and X are the primary co-monomer and cross-linking monomer, respectively. The primary co-monomers were methyl methacrylate (MMA), ethyl acrylate (EA) or butyl methacrylate. The cross-linking monomers were either butanediol diacrylate (BDDA) or ethyleneglycol dimethacrylate (EGDMA). The microgels were studied using scanning electron microscopy, photon correlation spectroscopy (PCS) and dynamic rheology measurements. Gel phase diagrams were also constructed. The particles swelled significantly at pH values greater than approximately 6.0. It was shown that poly(EA/MAA/X) microgels swelled more strongly than poly(MMA/MAA/X) microgels. Furthermore, greater swelling occurred for particles prepared using EGDMA than BDDA. Concentrated dispersions of all the microgels studied exhibited pH-triggered gel formation. It was found that the fluid-to-gel transitions for the majority of the six microgel dispersions investigated could be explained using

PCS data. In those cases, gelation was attributed to a colloidal glass transition. Interestingly, the microgels that were considered to have the highest hydrophobic content gelation occurred under conditions where little particle swelling was evident from PCS. The data presented show that gelled poly(EA/MAA/BDDA) and poly(MMA/MAA/EGDMA) microgel dispersions have the strongest elasticities at pH=7.

**Keywords** Microgel · pH-responsive particles · Gelation · Rheology

## Introduction

This article is dedicated to Prof. Haruma Kawaguchi in honour of his important contributions to colloid and polymer science. He has published many influential papers concerning microgels [1–4], which have included groundbreaking approaches such as the preparation of Janus microgels [5, 6]. In this work, we investigate pH-responsive microgels. These are [7, 8] cross-linked polymer particles that swell when the pH approaches the  $pK_a$  of the polymer that comprises the particles. The first water-dispersible responsive microgel was reported by Pelton and Chibante [9] in 1986. In previous work from our group [10], it was established that the height and mechanical properties of degenerated intervertebral discs could be restored by injection of poly(EA/MAA/BDDA) microgel followed by pH triggered swelling. (EA, MAA and BDDA are ethyl acrylate, methacrylic acid and butanediol diacrylate, respectively). In the present study, we investigate the effects of microgel particle composition on pH-triggered particle swelling and gel formation of concentrated microgel dispersions.

S. Lally · R. Bird · B. R. Saunders (✉)  
Biomaterials Research Group, School of Materials,  
The University of Manchester,  
Grosvenor Street,  
Manchester M1 7HS, UK  
e-mail: Brian.saunders@manchester.ac.uk

T. J. Freemont  
Tissue Injury and Repair Group, School of Medicine,  
Stopford Building, The University of Manchester,  
Oxford Road,  
Manchester M13 9PT, UK

Microgel number	poly (A/MAA/X)	Primary co-monomer (mol%)	MAA <sup>a</sup> (mol%)	$d_{\text{pH}=4}$ (nm)	$q_{\text{pH}=8}$ <sup>b</sup>	pH <sub>q=4</sub>	pHgel at $\varphi_p = 0.10$	$G'_{\text{max}}$ (Pa) <sup>c</sup>	$\text{p}K_a$ <sup>d</sup>
1A	MMA/MAA/BDDA	62	37	106	3.7	7.0	7.1	940	—
1B	MMA/MAA/EGDMA	62	37 (45.0)	103	11.1	6.7	6.7	1510	6.35
1B(L)	MMA/MAA/EGDMA	80	19 (23.0)	108	0.9	—	8.0	1930	7.60
2A	EA/MAA/BDDA	62	37 (37.0)	112	26.4	6.0	6.6	1640	6.70
2B	EA/MAA/EGDMA	62	37	76	156	5.7	6.2	300	—
3A	BMA/MAA/BDDA	54	45 (29.0)	104	1.8	—	6.0	220	8.20

**Fig. 1** Structures of MMA (a), EA (b), BMA (c), MAA (d), BDMA (e) and EGDMA (f)

## Experimental

### Preparation of microgels

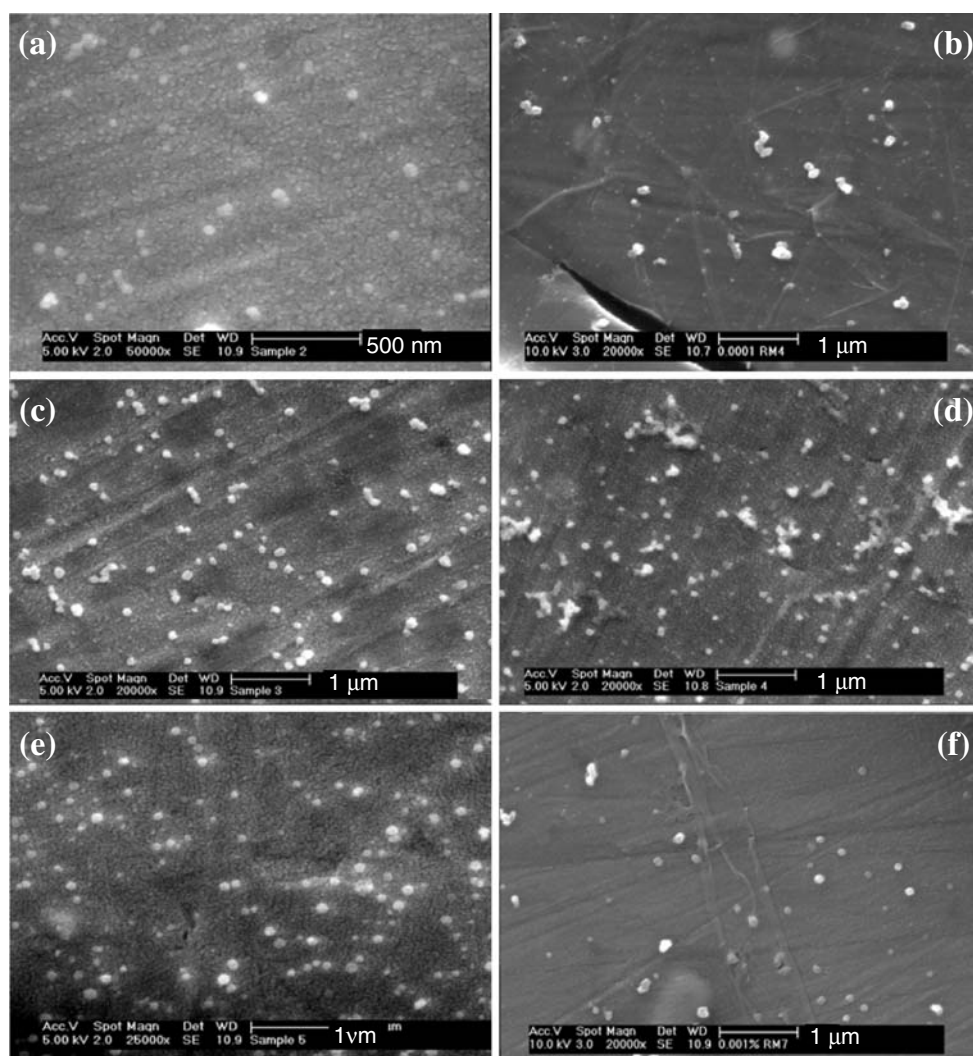
Table 1 shows a summary of the compositions for the microgels discussed in this work. All microgels were prepared using a seed-feed method. Microgel 2A was prepared using the method of Rodriguez et al. [19]. The following gives the preparation method used for microgel 1B (note that microgel 1B(L) was prepared using half the amount of MAA). Similar methods were used for the other microgels. A monomer mixture containing MMA (Aldrich, 99%, 143.5 g), MAA (Aldrich, 99%, 72.0 g) and BDDA (Aldrich, 98%, 2.2 g) was prepared and 12.5 % of the mixture added to a pre-purged, stirred solution of sodium dodecyl sulphate (SDS, BDH, 1.75 g in 500 g of water) which had been heated to 80 °C. The monomers were passed over an alumina column prior to use to remove inhibitor.  $K_2HPO_4$  (3 g of 7% solution in water) and 2.95 g

of a 5% ammonium persulfate (Aldrich, 98%) solution in water were immediately added whilst maintaining a nitrogen atmosphere. After appearance of a slight blue turbidity, the feed was commenced. An additional quantity of SDS solution (1.75 g SDS in 57.5 g of water) was added at this point and the remaining monomer mixture added at a continuous rate over a 90-min period. Additional ammonium persulfate (3.3 g of 5% solution in water) was added and the temperature maintained at 80 °C for a further 2 h. The microgel was extensively dialysed against Milli-Q quality water.

### Physical measurements

Photon correlation spectroscopy measurements were performed using a BI-9000 Brookhaven light scattering apparatus (Brookhaven Instrument Cooperation) fitted with a 20 mW HeNe and the detector was set at 90° scattering angle. A mixed pH-buffer system (0.1 M) was used to maintain the pH

**Fig. 2** SEM micrographs for the following microgels. **a** 1A, **b** 1B, **c** 2A, **d** 2B, **e** 3A and **f** 1B(L)



at specific values (below). The particle swelling ratio ( $q$ ) was calculated using Eq. 1:

$$q = \left[ \frac{d}{d_c} \right]^3 \quad (1)$$

where  $d$  is the hydrodynamic diameter and  $d_c$  is the average diameter of collapsed particles. In this work, we used the hydrodynamic diameter measured at pH=4 ( $d_{\text{pH}=4}$ ) for  $d_c$  (see Table 1).

Scanning electron microscopy (SEM) measurements were obtained using a Philips FEGSEM instrument. Fluid-to-gel phase diagrams were constructed by mixing known ratios of microgel with sodium hydroxide solution and then tested using tube inversion. Gels were considered to be present if the samples did not flow when the tube was inverted. Rheology measurements were performed using a Rheometrics RMS-800. A cone and plate measurement geometry was used. A frequency range of 0.01 to 15.9 Hz was employed. The strain used for these measurements was 10%.

## Results and discussion

### Microgel characterisation

A range of microgels were prepared in this work (Table 1). The structures of the co-monomers used are shown in Fig. 1. The structure of the primary monomer was changed from MMA to EA and butyl methacrylate (BMA) in order to probe this effect on the pH-dependent properties. We also investigated the effect of cross-linking monomer type by using BDDA or EGDMA. The nominal concentration of MAA within the microgel particles was also varied.

SEM was used to investigate particle morphology (Fig. 2). Spherical particles were clearly evident for each of the microgel dispersions with sizes in the region of approximately 70–100 nm. This range is consistent with the data obtained from photon correlation spectroscopy (PCS) measurements (Table 1). The PCS results were a much better measure of particle size than SEM. As will be shown below, the particles did not swell significantly until the pH exceeded approximately 6.0. It can be seen from Table 1 that all of the microgels have collapsed particle sizes ( $d_{\text{pH}=4}$ ) in the range of about 75 to 110 nm. This is consistent with previous work from our group [10] and other workers for microgel 2A [19].

### pH-triggered swelling of microgel particles

The pH-dependent swelling of the particles was investigated using PCS measurements (Fig. 3). Values of  $q$  measured at pH=8 ( $q_{\text{pH}=8}$ ) are shown in Table 1. All of the microgels

showed pH-triggered swelling of the particles to some extent. This begins at pH values greater than 4.0 and is significant at pH values above 6.0. Microgel 2A is used here as a well-studied reference system, and the behaviour observed is consistent with earlier results [10, 19]. The effective  $\text{p}K_a$  for this microgel was measured as 6.7 in our earlier work [16]. The ionicity (or degree of neutralisation) is given by the following equation [10]:

$$i = \frac{1}{1 + 10^{\text{p}K_a - \text{pH}}} \quad (2)$$

A pH of 6.7 should correspond to  $i=0.5$ . From the data shown in Fig. 3, this corresponds to the pH region at which  $q$  increases substantially. Therefore, it is reasonable to associate the region of major particle swelling for each microgel with its effective  $\text{p}K_a$ . The  $\text{p}K_a$  values for several of the other microgels are also shown in Table 1. Interestingly, microgels 1B(L) and 3A had the highest  $\text{p}K_a$

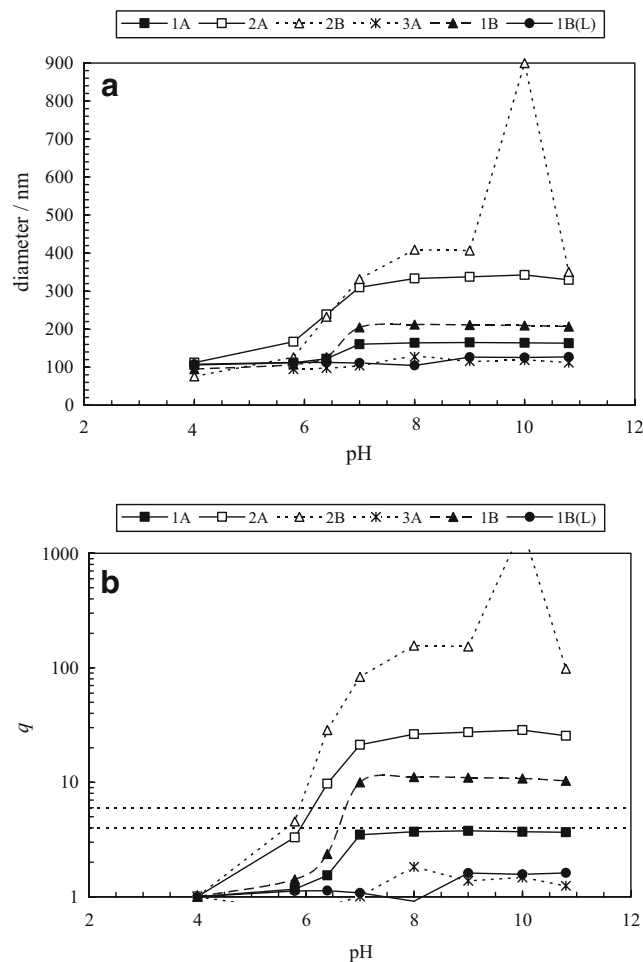


**Fig. 3** Variation of hydrodynamic diameter (a) and swelling ratio (b) with pH for various microgels. The horizontal lines shown in b correspond to  $q$  values of 4.0 and 6.0 (see text)



values. These microgels are considered to have the most hydrophobic compositions.

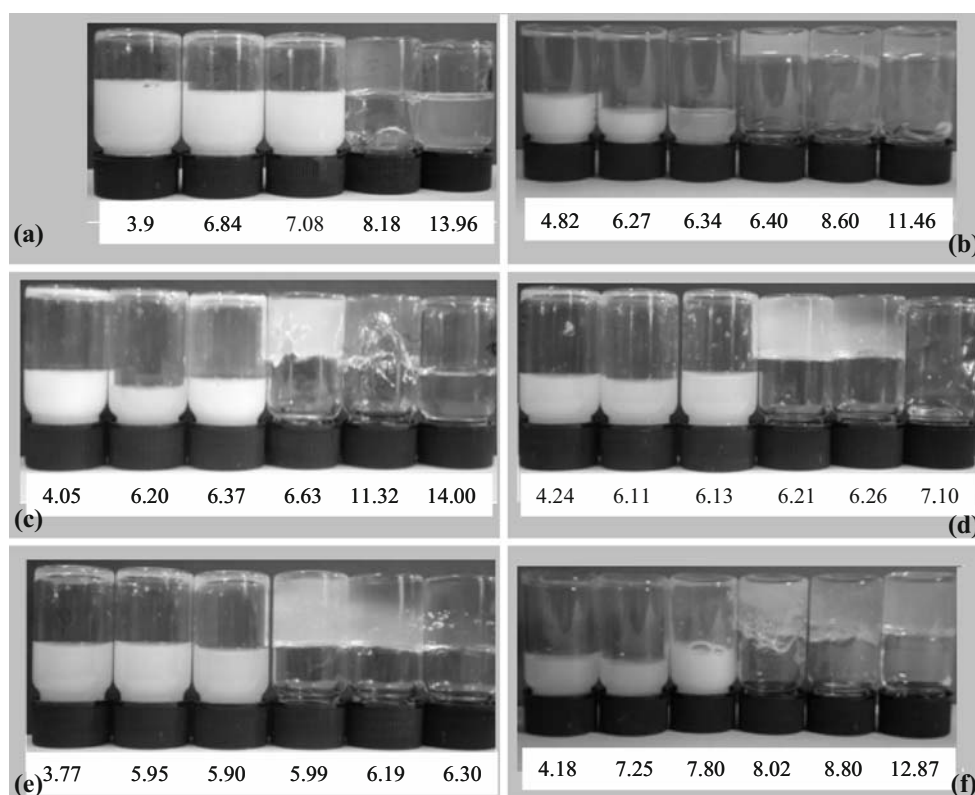
It can also be seen from Fig. 3 and Table 1 that the microgels containing EA exhibit greater extents of swelling (as judged by  $q$ ) than those containing MMA (the spike at pH=10 for Microgel 1B is not due to normal particle swelling and will be discussed below). This is an interesting trend and has not been reported before to our knowledge. A difference in cross-link densities between the particle types is possible such that EA promotes lower values. However, this is not considered likely because the relative order of  $q$  values (greatest for EA) is preserved (Table 1) for microgels prepared using structurally different cross-linking monomers (BDDA cf. EGDMA). Another explanation is required. We propose that the differences in swelling for these microgels is related, in part, to the respective glass transition temperatures ( $T_g$ ) of the primary polymers.  $T_g$  values were determined using differential scanning calorimetry for microgels 1A, 2A and 3A. The  $T_g$  values determined from those data were, respectively, 143.5, 26.0 and 50.0 °C, respectively. The values are higher than, but in the same order, as those for the homopolymers. The  $T_g$  values for poly(MMA), poly(EA) and poly(BMA) are approximately [24] 99, −23 and 23 °C, respectively. The  $T_g$  value for [24] poly(MAA) is approximately 228 °C. It is the incorporation of MAA that is responsible for the higher  $T_g$  values of the microgels compared to the homopolymers. Furthermore, the  $T_g$  is related to chain flexibility, and it is

proposed that a lack of conformational flexibility for the MMA-rich chains restricts the extent of particle swelling that can be achieved. This idea, however, cannot explain the low swelling for microgel 3A. Presumably, that is due in part to the hydrophobic nature of BMA (discussed below).

It can also be seen from Fig. 3 and Table 1 that microgels containing EGDMA swell more than those containing BDDA. Microgel 2B particles partially dissolved at pH=10, which is an indication of insufficient cross-linking monomer incorporation at the particle periphery. It is therefore reasonable to suggest that EGDMA results in a lower shell cross-linking density than BDDA. The EGDMA cross-linking monomer should be more reactive than BDDA, being a methacrylate, and can be expected to be incorporated into the core of the particles more effectively, which would lead to a relative lack of cross-linking monomer at the particle periphery.

A third trend from Fig. 3 and Table 1 is that microgel 3A exhibits the least pH-triggered swelling of the microgels. The primary monomer is the most hydrophobic of all used in this work. Presumably, hydrophobic domains may form within the particle (acting as associative cross-links) which oppose pH-triggered swelling. It can be seen from Table 1 that the actual mol% MAA incorporated into the microgel 3A particles, as determined by potentiometric titration, was relatively low (29.0 mol%) compared to the other microgels. This may contribute to the relatively low extent

**Fig. 4** Images of fluids and gels obtained at different pH values. The samples were: **a** 1A, **b** 1B, **c** 2A, **d** 2B, **e** 3A and **f** 1B(L)



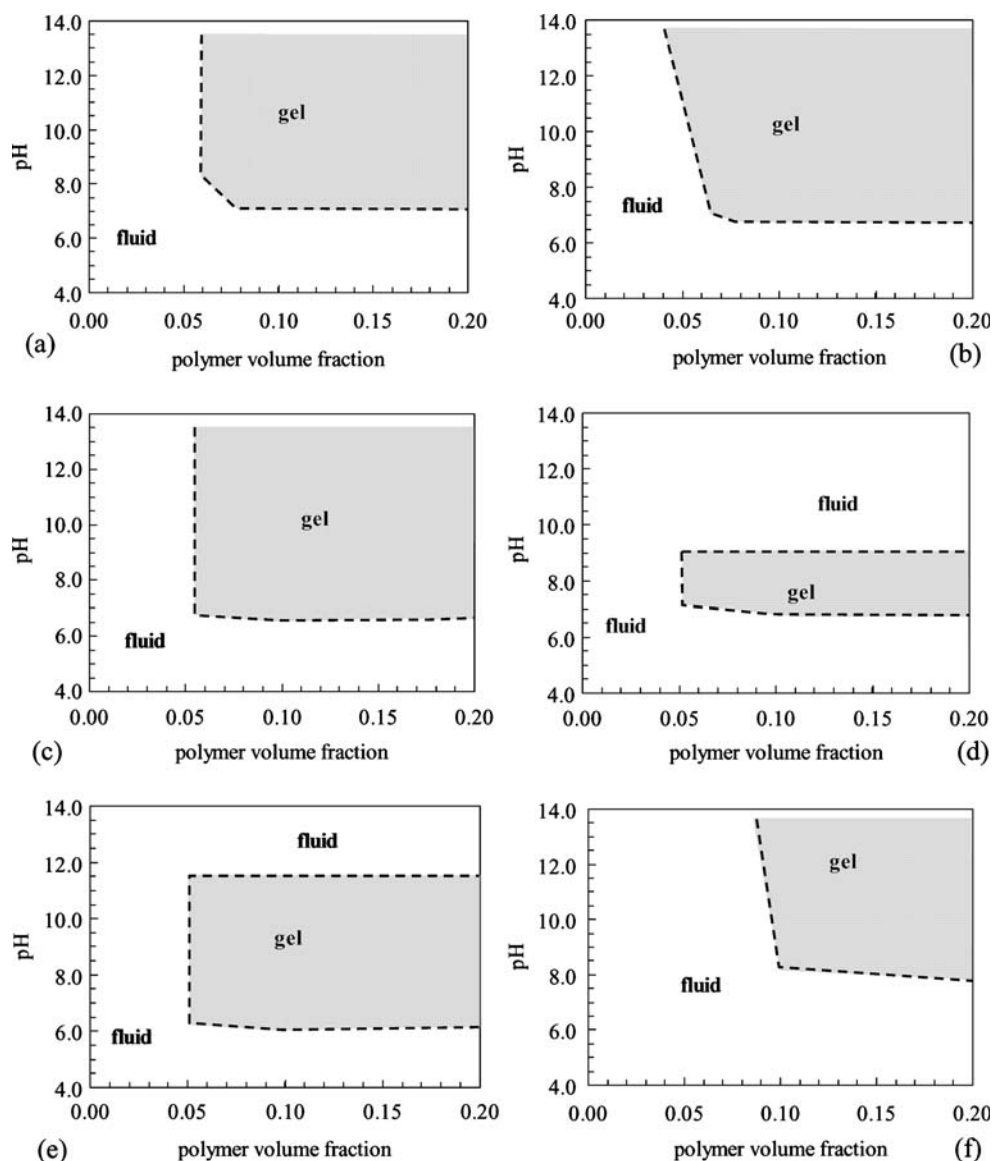
of pH-triggered swelling observed for microgel 3A compared to the other systems.

A final trend from the data shown in Fig. 3 is that the  $q$  value decreases with decreasing MAA content, i.e. microgel 1B(L) swells much less than microgel 1B. This is expected and can be explained in a straightforward manner using electrostatic repulsion arguments or considering the osmotic pressure associated with mobile ions. Furthermore, microgel 1B(L) seems to have a higher effective  $pK_a$  than microgel 1B because it can be seen from Fig. 3 that swelling does not begin until the pH exceeds 8.0. This is supported by the relatively high  $pK_a$  determined for this microgel (Table 1.) It has been noted in related work [25] involving particles containing MAA that increasing levels of hydrophobic co-monomers increases the effective  $pK_a$ .

pH-triggered gelation of concentrated microgel dispersions

In order to assess the gel-forming properties of the microgel dispersions, fluid-to-gel phase transitions were investigated using the tube inversion method. Images of selected fluids and gels are shown in Fig. 4. These images were taken using concentrated dispersions with a particle volume fraction,  $\phi_p$ , of 0.10. These types of gels have been assumed to form [15] because of steric confinement of swollen particles. The gels that form result from swelling of the particles to the point where a critical  $\phi_p^*$  value is reached [26], i.e. when the effective microgel particle volume fraction,  $\phi_{eff(m)} = \phi_p^*$ . The particles then become sterically confined by their neighbours. Strictly speaking, the gelled state is an equilibrium property of the microgel dispersion caused by steric confinement of swollen particles. It is considered as a

**Fig. 5** Gelation phase diagrams for various microgels. The systems are: **a** 1A, **b** 1B, **c** 2A, **d** 2B, **e** 3A and **f** 1B(L)



colloidal glass transition. The gelation is reversible because dilution with water of the same pH reduced  $\phi_p$  to less than  $\phi_p^*$  and a gel-to-fluid transition occurred.

Tube inversion measurements were used to construct phase diagrams (Fig. 5) for all of the microgel dispersions. A key parameter is the minimum pH at which a gel forms ( $\text{pH}_{\text{gel}}$ ) when  $\phi_p=0.10$ . An interesting trend can be seen (Table 1) is that  $\text{pH}_{\text{gel}}$  for the poly(A/MAA/X) microgels increases in the order  $X = \text{BMA}, \text{EA}, \text{MMA}$ . Furthermore,  $\text{pH}_{\text{gel}}$  is smaller for  $X = \text{EGDMA}$  than when  $X = \text{BDDA}$ . The third trend is that  $\text{pH}_{\text{gel}}$  is much higher for microgel 1B(L) than for 1B.

The relationship between  $\phi_{\text{eff(m)}}$  and  $\phi_p$  is given by Eq. 3:

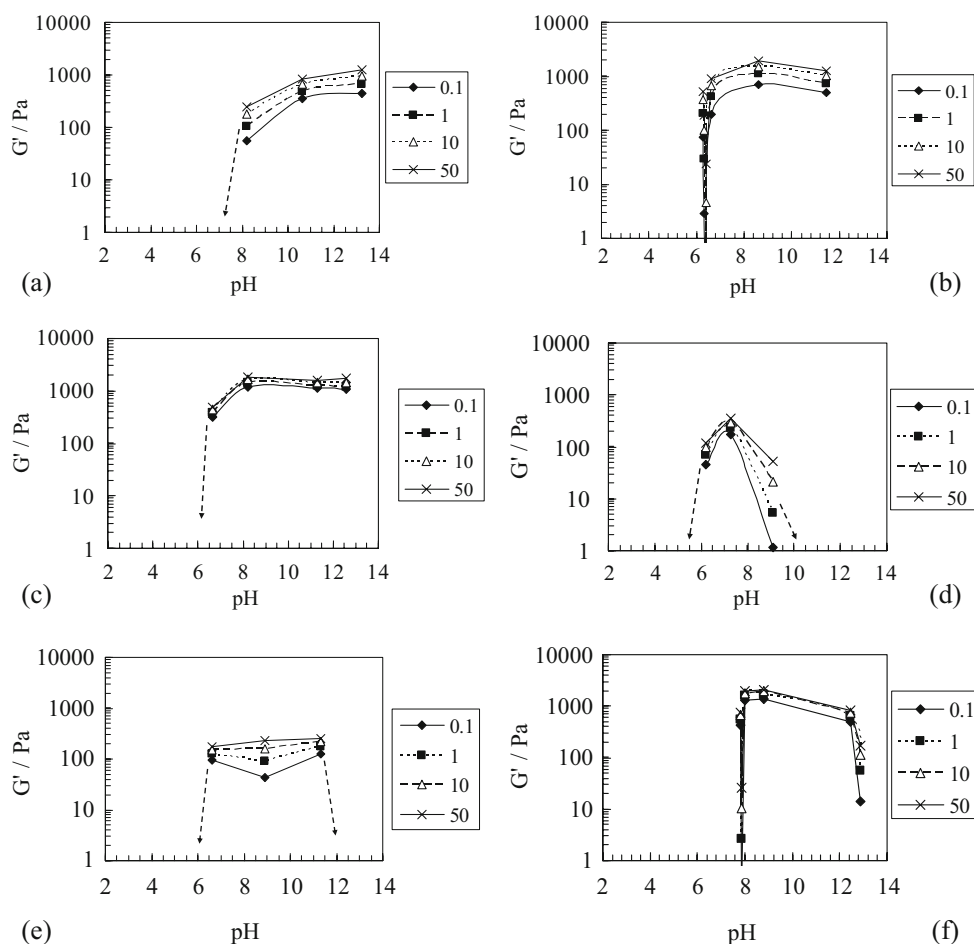
$$\phi_{\text{eff(m)}} = q\phi_p \quad (3)$$

It was suggested previously that a critical  $\phi_p^*$  of about 0.4 to 0.6 applied for microgel 1B dispersions [15]. This was tested for all of the microgels in the present work using the data shown in Fig. 3b. At  $\phi_p=0.10$ , the critical  $q$  values at which gels form should be between 4.0 and 6.0. Table 1 shows the pH at which  $q=4.0$  ( $\text{pH}_{q=4}$ ) for the microgels. It can be seen that there is reasonable agreement between  $\text{pH}_{q=4}$

and  $\text{pH}_{\text{gel}}$  for four of the six microgels investigated. This suggests that gel formation can be explained using the concept of a colloidal glass transition due to steric confinement for those systems. However, it must be noted that increasing amounts of NaOH added to increase the pH of the dispersions causes the ionic strength to increase considerably. This will cause some de-swelling of the microgel particles. Therefore, the  $\text{pH}_{q=4}$  values shown in Table 1 should be considered as minimum values.

It is, however, noteworthy that two of the microgel dispersions [microgels 1B(L) and 3A] form gels when the  $q$  values are much less than 4.0; therefore,  $\phi_{\text{eff(m)}}$  is much less than  $\phi_{\text{eff(m)}}^*$  when these gels form. This would indicate that gelation for those systems is a result of another mechanism. The fact that some swelling occurs for these systems (Fig. 3b) in the vicinities of the respective  $\text{pH}_{\text{gel}}$  values (Table 1) indicates that neutralisation of the RCOOH groups must occur. However, in both systems, the hydrophobic interactions due to microdomain formation by the principal monomer (BMA or MMA) presumably restrict the extents of swelling. It is proposed that the result is a highly charged microgel with strong electrostatic repulsion between particles (by contrast, the charge density is reduced

**Fig. 6** Variation of  $G'$  with pH at selected  $\omega$  values in rad/s (see legend) for concentrated microgel dispersions ( $\phi_p=0.10$ ). The systems investigated were: **a** 1A, **b** 1B, **c** 2A, **d** 2B, **e** 3A and **f** 1B(L)



somewhat in a microgel that swells). This could result in a gel by virtue of repulsive interparticle interactions.

Considering the phase diagrams for microgels 2B and 3A (Fig. 5d, e), it can be seen that gel-to-fluid transitions are evident at high pH. In the case of microgel 2B, this is attributed to partial particle dissolution at high pH, as was observed by PCS measurements (Fig. 3). In the case of 3A, however, no evidence of particle dissolution can be found from PCS measurements, although the maximum pH of those measurements was slightly less than the gel-to-fluid transition pH (of approximately 11.5). A high ionic strength, due to addition of NaOH, would decrease electrostatic repulsion and may be the cause of the gel-to-fluid transition in that case.

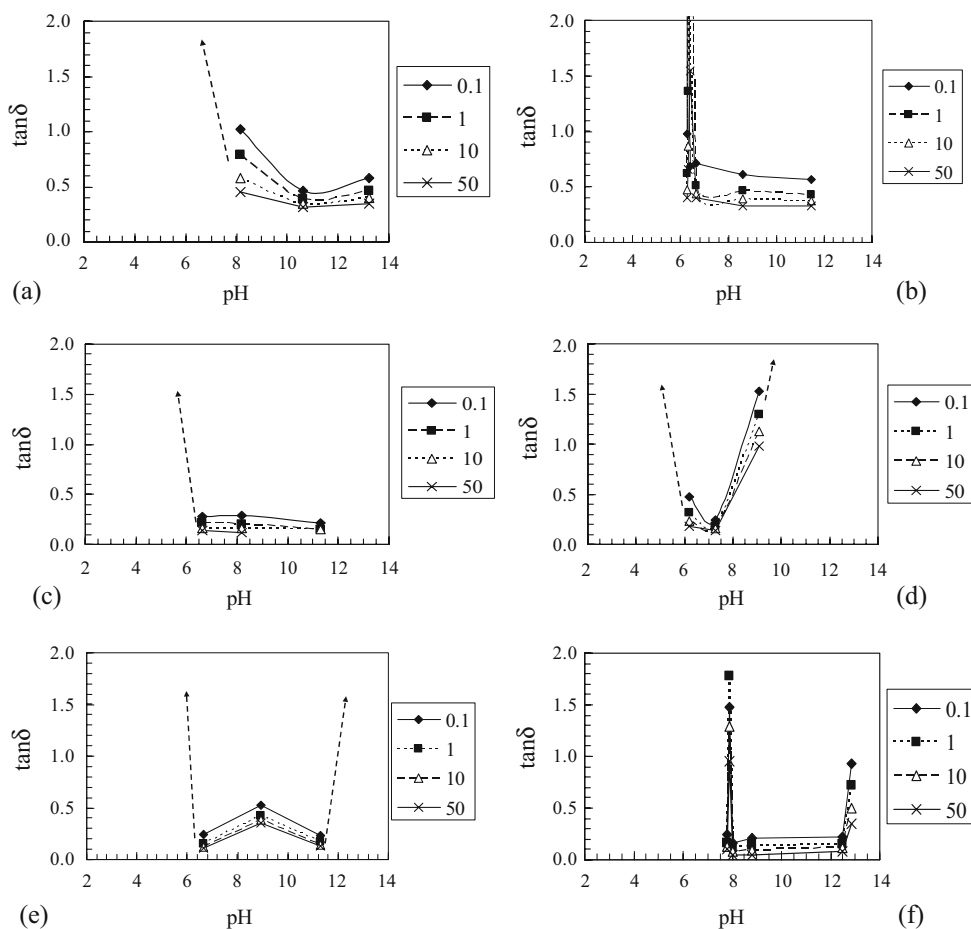
#### Rheological studies of concentrated microgel dispersions

The viscoelastic properties of the gels were investigated using dynamic rheology measurements at room temperature. Data for  $G'$  (elastic modulus) and  $\tan\delta$  ( $\delta=G''/G'$ ,  $G''$  is the loss modulus) are plotted in Figs. 6 and 7 as a function of pH. All of these data were obtained using  $\phi_p=0.10$ . Data at

selected oscillation frequencies,  $\omega$ , are presented in these figures. This enables the frequency dependence of the parameters to be assessed. The maximum values for  $G'$  obtained,  $G'_{\max}$ , are a measure of maximum gel elasticity and are shown in Table 1.

Generally, a fluid is indicated by low  $G'$  values and  $\tan\delta$  values greater than 1.0. Conversely, a gel is indicated by  $\tan\delta \leq 1.0$  and increased  $G'$  values. The data shown in Figs. 6 and 7 are consistent with the respective phase diagrams (Fig. 5) and show the fluid-to-gel or gel-to-fluid transitions. Another criteria for a gel is frequency-independent  $\tan\delta$  values [27]. However, all the gels show frequency-dependent  $\tan\delta$  values (Fig. 7). This is a common observation for physical gels as discussed by Seetapan et al. [28] The frequency dependence of the  $\tan\delta$  values may originate from the non-permanent nature of the networks that are responsible for our gels or from a disordered arrangement of swollen particles within the gels. The latter comment takes into account the fact that our gels result from upon a rapid increase in  $\phi_{\text{eff}(m)}$ . A frequency-independent  $\tan\delta$  may be expected in physical gels where a self-similar structure occupies the entire gel volume. However, in the

**Fig. 7** Variation of  $\tan\delta$  with pH at selected  $\omega$  values in rad/s (see legend) for concentrated microgel dispersions ( $\phi_p=0.10$ ). The systems investigated were: **a** 1A, **b** 1B, **c** 2A, **d** 2B, **e** 3A and **f** 1B(L)





case of a less ordered structure, a range of local environments can be envisaged, some of which may have a large viscous component.

It can be seen from Fig. 6 and Table 1 that the poly(A/MAA/X) (A = MMA or EA) gels have highest  $G'$  values. The strongest and weakest gelled microgel dispersions, as judged by  $G'$ , are microgels 1B(L) and 3A, respectively. The origin of this difference is not clear at this stage and requires a more detailed rheological study. It is noteworthy, however, that for both of these systems, there are noticeable decreases in  $G'$  at higher pH values (Fig. 6e, f). We suggest that this is due to a gel-to-fluid transition as a result of the increased ionic strength (due to NaOH addition) and concurrent decreased electrostatic repulsion. This behaviour is similar to that observed for microgel 2B (Figs. 6d and 7d), which also exhibited a maximum for  $G'$  with respect to pH. However, in that case, the decrease of  $G'$ , and increase of  $\tan\delta$ , at high pH values is attributed to partial particle dissolution. This was evident from the PCS data (Fig. 3).

An important consideration for our intervertebral disc repair programme is the viscoelastic properties of the gelled microgel dispersions in the vicinity of pH=7.0. It can be seen from Fig. 6 that the gels with the highest  $G'$  values at pH=7.0 are microgels 1B and 2A. The viscoelastic properties of each of these gels are not greatly different. This result suggests that for these gelled microgel dispersions, the conformational flexibility is not a factor that governs gel elasticity.

## Conclusions

This work has investigated in detail the pH-triggered particle swelling and gelation of microgel dispersions containing MAA. It is the first study of its type to systematically investigate the effect of microgel composition on particle swelling and gelation properties for these dispersions. The work has demonstrated that poly(EA/MAA/X) particles swell more strongly than poly(MMA/MAA/X) particles. This may be due to reduced poly(MMA) conformational mobility. The most hydrophobic microgels, microgels 1B(L) and 3A, swelled least. It was also found that microgels containing EGDMA swelled more than those prepared using BDDA. There were two distinct gel types identified in this work. Four of the six systems studied gave gels due to steric confinement of the particles, and the pH values at which fluid-to-gel transitions occurred could be explained using their pH-dependent particle sizes (from PCS). In addition, the two most hydrophobic microgels gave gels when  $\phi_{\text{eff(m)}}$  was much less than those values.

The work has clearly shown that the gels that are most suited for use in the body, at least in terms of the elastic properties, are microgels 2A and 1B. The latter system is preferred for potential use in vivo because it is based on

components that have already been used as biomaterials [23]. The application of microgels within the body for soft tissue repair is an area that is currently being investigated at Manchester [10] and elsewhere [29].

**Acknowledgements** We are grateful to the Enterprise, Medicine and Materials schools of the University of Manchester for funding this project. We are also grateful to Mike Faulkner for assisting with SEM. We are also grateful to Prof. Peter Lovell for access to the PCS instrument. We thank the reviewers of this manuscript for their insightful comments.

## References

- Jeenanong A, Kawaguchi H (2008) *Colloids Surf A* 315:232
- Kawaguchi H (1996) *Frontiers Biomed Biotech* 3:157
- Ni HM, Kawaguchi H, Endo T (2007) *Colloid Polym Sci* 285:873
- Ni HM, Kawaguchi H, Endo T (2007) *Colloid Polym Sci* 285:819
- Suzuki D, Tsuji S, Kawaguchi H (2007) *J Am Chem Soc* 129:8088
- Suzuki D, Kawaguchi H (2006) *Colloid Polym Sci* 284:1471
- Saunders BR, Vincent B (1999) *Adv Colloid Interface Sci* 80:1
- Saunders BR, Vincent B (2002) *Encyclopedia of surface and colloid science* (edited by Hubbard A). Marcel-Dekker, NY, p 4544
- Pelton RH, Chibante P (1986) *Colloids Surf* 120:247
- Saunders JM, Tong T, Le Maitre CL, Freemont TJ, Saunders BR (2007) *Soft Matter* 3:486
- Saunders BR, Laajama N, Daly E, Teow S, Hu X, Stepto R (2009) *Adv Colloid Interface Sci* (in press)
- Fernandez-Nieves A, Fernandez-Barbero A, Vincent B, de las Nieves FJ (2000) *Macromolecules* 33:2114
- Brugger B, Richtering W (2008) *Langmuir* 24:7769
- Hoare T, Pelton RH (2006) *Langmuir* 22:7342
- Lally S, Mackenzie P, LeMaitre CL, Freemont TJ, Saunders BR (2007) *J Colloid Interface Sci* 316:367
- Dalmont H, Pinprayoon O, Saunders BR (2008) *Langmuir* 24:2834
- Cornelius VJ, Snowden MJ, Mitchell JC (2007) *Proceedings of SPIE—The International Society for Optical Engineering*, 64130Y/1 6417
- Morris GE, Vincent B, Snowden MJ (1997) *J Colloid Interface Sci* 190:198
- Rodriguez BE, Wolfe MS, Fryd M (1994) *Macromolecules* 27:6642
- Singh N, Lyon LA (2008) *Colloid Polym Sci* 286:1061
- Hazot P, Delair T, Elaissari A, Chapel J-P, Pichot C (2002) *Colloid Polym Sci* 280:637
- Tan BH, Tam KC, Lam YC, Tan CB (2005) *Adv Colloid Interface Sci* 113:111
- Freemont TJ, Saunders BR (2008) *Soft Matter* 4:919
- Brandrup J, Immergut EH, Grulke EA, Abe A, Bloch DR (1999) *CRC polymer handbook*, 4th edn. Wiley, New York
- Pinprayoon O, Groves B, Saunders BR (2008) *J Colloid Interface Sci* 321:315
- Prasad V, Trappe V, Dinsmore AD, Segre PN, Cipolletti L, Weitz DA (2003) *Faraday Discuss* 123:1
- Winter HH, Chambon F (1986) *J Rheol* 30:367
- Seetapan N, Mai-ngam K, Plucktaveesak N, Sirivat A (2006) *Rheol Acta* 45:1011
- Jia X, Yeo Y, Clifton RJ, Jiao T, Kohane DS, Kobler JB, Zeitel SM, Langer R (2006) *Biomacromolecules* 7:3336